Article

Discovery Medicine 2025; 37(202): 2687–2701
https://doi.org/10.24976/Discov.Med.202537202.225

IL-25 Attenuates Rheumatoid Arthritis via Inhibition of the TLR4/NF-κB/NLRP3 Signaling Pathway

Jinyue Lu[1,2], Jiayao Hao[1,2], Jianxiong Zheng[1,2], Haiyang Liao[1,2], Chunhua Liu[1,2], Haili Shen[1,*]

[1]Department of Rheumatology, The Second Hospital & Clinical Medical School, Lanzhou University, 730030 Lanzhou, Gansu, China
[2]The Second Hospital & Clinical Medical School, Lanzhou University, 730030 Lanzhou, Gansu, China
*Correspondence: shenhl@lzu.edu.cn (Haili Shen)
Submitted: 26 June 2025 Revised: 5 September 2025 Accepted: 19 September 2025 Published: 20 November 2025

Background: Persistent inflammation contributes to the progression of rheumatoid arthritis (RA); however, the exact molecular mechanisms underlying inflammation in RA are yet to be fully elucidated. Interleukin-25 plays a crucial role in host defense and the pathogenesis of inflammatory diseases. Its specific contribution to RA progression requires further investigation.
Methods: RA-FLSs were treated with tumor necrosis factor-α (TNF-α) to simulate the inflammatory response in the synovium. Furthermore, changes in inflammatory response and bone destruction indicators were assessed after Interleukin-25 (IL-25) intervention. The collagen-induced arthritis (CIA) mouse model was successfully constructed to evaluate the impact of IL-25 on joint inflammation and erosion.
Results: The expression levels of IL-25 were significantly elevated in the synovial tissues of both RA patients and CIA mouse models compared to controls ($p < 0.05$). *In vitro*, IL-25 pretreatment substantially suppressed TNF-α-induced upregulation of interleukin-1β (IL-1β), interleukin-6 (IL-6), high mobility group box-1 protein (HMGB1), matrix metalloproteinase-3 (MMP-3), toll-like receptors 4 (TLR4), and NOD-like receptor thermal protein domain-associated protein 3 (NLRP3) in RA-FLSs ($p < 0.05$, $p < 0.01$, $p < 0.001$), and suppressed nuclear factor kappa-B (NF-κB) signaling pathway by reducing p-P65 and p-IκBα protein levels ($p < 0.001$). *In vivo*, IL-25 negatively regulated joint inflammation and reduced the degree of bone erosion in mice ($p < 0.01$, $p < 0.0001$).
Conclusion: Elevated IL-25 levels exert anti-inflammatory effects both *in vitro* and *in vivo* and alleviate RA progression by inhibiting the TLR4/NF-κB/ NLRP3 signaling pathway.

Keywords: rheumatoid arthritis; IL-25; tumor necrosis factor-α; NF-κB signaling pathway

Introduction

Rheumatoid Arthritis (RA) is a chronic systemic autoimmune disease characterized by symmetric polyarthritis, synovial hyperplasia, and progressive bone and cartilage destruction, ultimately resulting in disability and a substantial decline in quality of life [1]. It is a multifactorial disease with complex pathogenesis, involving aberrant activation of immune cells, cytokine networks, and signaling pathways. Targeted cytokine therapies have become effective treatments for RA [2]. A key contributor to disease progression is the fibroblast-like synoviocytes (FLS) within the RA synovium, which exhibit hyperproliferative, invasive, and tumor-like properties, secreting pro-inflammatory mediators and matrix metalloproteinases (MMPs) that drive pathogenesis [3]. Increasing evidence indicates that the hyperactivation of RA-FLS plays a crucial role in perpetuating RA pathogenesis [4–7].

Furthermore, tumor necrosis factor-α (TNF-α) is a key regulator in the progression of RA. It triggers a cascade of pro-inflammatory cytokines, including IL-1β, IL-6, and IL-8, thereby establishing an inflammatory network [8]. In RA, TNF-α not only directly induces FLS proliferation and MMP secretion, leading to cartilage degradation and bone erosion, but also stimulates osteoclast differentiation, which exacerbates bone resorption and aggravates bone destruction [9]. Additionally, TNF-α promotes inflammatory cell infiltration by upregulating vascular endothelial adhesion molecules and induces angiogenesis, further amplifying synovial inflammation, a hallmark event in RA progression [10]. Mechanistically, TNF-α activates key signaling pathways, such as NF-κB and MAPK, which further perpetuate chronic synovitis [11,12].

Interleukin-25 (IL-25), also known as IL-17A, is a structurally distinct member of the IL-17 family, sharing only 16–20% amino acid sequence homology with IL-17A. Unlike IL-17A, which has a well-recognized pro-inflammatory role in RA, IL-25 has been primarily investigated for its role in regulating type 2 immunity, particularly in parasitic infections and allergic responses [13,14]. Pre-

vious studies suggest that IL-25 exerts anti-inflammatory effects by suppressing Th17 responses [15–17]. In our earlier study, we reported that IL-25 levels were significantly elevated in the serum of patients with RA and partially inhibited IL-17-induced MMP-3 expression in RA-FLS. These observations suggest that IL-25 may serve as an anti-inflammatory mediator in RA, warranting further investigation into its regulatory role in disease progression [18].

This study evaluated IL-25 levels in human synovium and fluid, examined its potential role in modulating inflammation, invasion, and migration of RA synovial fibroblasts, and identified changes in associated signaling pathway proteins. Additionally, upon establishing a collagen-induced arthritis (CIA) model, we investigated changes in IL-25 expression and explored its underlying mechanisms of action in an animal model.

Materials and Methods

Clinical Subjects

Synovial fluid samples were collected from 11 RA patients (classified following the 2010 ACR/EULAR criteria) and 6 age- and sex-matched osteoarthritis (OA) controls. Individuals with comorbid conditions were excluded. Disease activity was stratified using DAS28-CRP: low activity (LRA, DAS28-CRP $\leq$5.1, n = 5) and high activity (HRA, DAS28-CRP >5.1, n = 6). Furthermore, synovial tissue samples were obtained from 3 RA and 3 OA patients undergoing knee arthroplasty. The study protocol received approval from the ethics committee of Lanzhou University Second Hospital (protocol No: 2025A-717).

Isolation and Culture of Synovial Fibroblasts

Synovial tissue samples collected from RA and OA patients during surgery were immediately transferred to a sterile workstation. The tissue was thoroughly rinsed with phosphate-buffered saline (PBS) and meticulously dissected into 1–2 mm fragments using sterile surgical scissors. These tissue fragments were cultured in high-glucose DMEM medium (6124370, Gibco, NY, USA) and incubated at 37 °C with 5% CO_2 for 1 hour. Following incubation, the medium was replaced with fresh complete DMEM. The suspension containing synovial fibroblasts was centrifuged at 2000 rpm for 15 minutes. After discarding the supernatant, the cell pellet was gently resuspended in fresh complete medium and transferred to culture conditions.

The third-generation fibroblasts under optimal growth conditions were seeded onto round glass slides. Upon reaching approximately 60% confluence, the cells were thoroughly washed with PBS, fixed with paraformaldehyde for 20 minutes, permeabilized with 3% Triton X-100 for 20 minutes, and then blocked with sheep serum (G1208, Servicebio, Wuhan, China) for 30 minutes. For immunofluorescence staining, the cells underwent overnight incubation at 4 °C with a Vimentin primary antibody (ab92547, Abcam, Cambridge, MA, USA). The next day, the cells were incubated with fluorescent secondary antibody (ab150089, Abcam, Cambridge, MA, USA) for 2 hours. Nuclei were counterstained with 4′,6-diamidino-2-phenylindole (DAPI, C1005, Beyotime, Shanghai, China) for 20 minutes, and cells were then fixed with gum. Cell morphology and Vimentin protein expression were observed under a fluorescence microscope to confirm cell type and purity.

Fibroblasts between passages 3 and 6 were selected for subsequent experiments. Cell cultures were confirmed as mycoplasma negative and authenticated using short tandem repeat (STR) profiling, which confirmed cell source and purity, minimizing the risk of cross-contamination. Cell identification was based primarily on morphology, Vimentin expression, and functional characteristics; however, CD55 marker confirmation was not used, which is a limitation of the research.

Establishment of Mouse Model and Treatment

The arthritis induction rate of DBA/1 mice is approximately 80–100% [19]. Therefore, for model induction, all DBA/1 mice, around 2 months old and weighing 18–20 g, were housed under pathogen-free conditions. The mice were sourced from Beijing Huafukang Biotechnology (License No. SCXK, Beijing, 2019-0008). To induce arthritis, type II collagen was emulsified with Complete Freund's Adjuvant at equal ratios. The nine mice were randomly divided into three experimental groups (n = 3): control, disease model, and treatment.

Collagen-induced arthritis was successfully established in six mice of the model and treatment groups, as confirmed by joint swelling. Arthritis indices were monitored and recorded daily. On day 21, both groups received a booster immunization. Beginning 2 days after the booster immunization, the model group received daily intraperitoneal injections of saline, whereas the treatment group received recombinant mouse IL-25 (1 μg/kg/day, 50138-M07H, Sino Biological, Beijing, China) for 5 consecutive days [20]. Clinical indicators, including hind paw and joint skin color, temperature, infection status, hind foot mobility, and joint swelling, were observed throughout the experiment.

All procedures involving animals were approved by the Ethics Committee of Lanzhou University Second Hospital (Ethics Approval No. D2025-473). At the end of the experiment, the mice were humanely euthanized under anesthesia by intraperitoneal injection of 3% phenobarbital (180 mg/kg), and tissue samples were then collected for subsequent analysis.

Hematoxylin and Eosin Staining

Synovial tissue samples were fixed in 4% paraformaldehyde, embedded in paraffin, and sectioned into 4 μm slices. Following standard histological

procedures, the tissue sections were oven-baked, deparaffinized, and rehydrated before hematoxylin and eosin (H&E) staining. Afterward, the samples were dehydrated using a graded alcohol series, cleared with xylene, and mounted with neutral resin for microscopic examination (DM3000, Leica, Germany).

Immunohistochemical Staining (IHC)

Paraffin-embedded human knee joint tissue samples were deparaffinized, followed by antigen retrieval using citrate buffer. Subsequently, the sections were subjected to DAB staining and counterstained with hematoxylin. After dehydration through a graded alcohol series, the samples were resin-mounted and examined using a fluorescence microscope (Olympus, Japan).

Enzyme-Linked Immunosorbent Assay (ELISA)

The levels of inflammatory cytokines were evaluated in synovial fluid samples and RA-FLS supernatants using commercially available ELISA kits: IL-25 (CSB-E11715h, Huamei, Wuhan, China, range: 62.5.25–4000 pg/mL), IL-6 (KE00139, San Ying, Wuhan, China, range: 7.8–500 pg/mL), and IL-1β (KE00021, San Ying, Wuhan, China, range: 3.9–250 pg/mL), following the manufacturer's instructions. All samples were analyzed in triplicate.

Cell Counting Kit-8 Assay

RA-FLSs were seeded in a 96-well plate at a density of 10,000 cells per well and allowed to adhere overnight. Based on pre-experimental results and previous studies [17,20,21], the cells were treated with varying concentrations of IL-25 (10, 50, and 100 ng/mL; C792, Novoprotein, China) and TNF-α (50 ng/mL, ADI-908-066-010, Xinbosheng, China) for 24 hours. After treatment, 10 µL of Cell Counting Kit-8 (CCK-8) reagent (BS350A, Biosharp, Guangzhou, China) was added to each well and incubated at 37 °C. Finally, absorbance was measured at 450 nm to determine cell viability.

Immunofluorescence Staining

RA-FLSs were seeded in 24-well plates at a density of 50,000 cells per well and allowed to adhere overnight. Following a 24-hour treatment with varying concentrations of IL-25 and TNF-α, the cells were washed three times with PBS and fixed in 4% paraformaldehyde for 30 minutes. After that, the cells were incubated overnight at 4 °C in a humidified environment with primary antibodies targeting TLR4 (GB11519-100, Servicebio, China, Dilution ratio 1:200), phosphorylated IκBα (ab32518, Abcam, Cambridge, MA, USA, Dilution ratio 1:200). The next day, the cells underwent a 1-hour incubation at room temperature with secondary antibodies (ab150089, Abcam, USA Dilution ratio 1:5000). After additional PBS washes, nuclei were counterstained with DAPI-containing anti-fade medium. The cells were then mounted and examined under a fluorescence microscope.

Quantitative Real-Time Polymerase Chain Reaction

The expression levels of interleukin-1 beta (*IL-1β*), interleukin-6 (*IL-6*), interleukin-8 (*IL-8*), matrix metalloproteinase-3 (*MMP-3*), C-C motif chemokine ligand 2 (*CCL-2*), interleukin-10 (*IL-10*), and transforming growth factor-beta (*TGF-β*) were assessed using quantitative reverse transcription polymerase chain reaction (*qRT-PCR*). Total RNA was isolated from RA-FLS using Trizol reagent (Invitrogen, Carlsbad, CA). To ensure purity, genomic DNA was eliminated before reverse transcription. RNA was then reverse transcribed into complementary DNA (cDNA) utilizing a PrimeScript RT kit with integrated gDNA removal (Takara Bio, Japan). qRT-PCR was performed with SYBR Green quantitative polymerase chain reaction (qPCR) Master Mix (Takara Bio, Japan) on a Bio-Rad CFX96 thermal cycler (BioRad, Hercules, CA, USA). Target gene expression levels were normalized to the housekeeping gene β-actin. Relative expression was determined using the $2^{-\Delta\Delta Cq}$ method. Primers used in qPCR are given in Table 1.

Table 1. A list of primers used in qPCR.

Gene	Primer Sequence (5′ to 3′)
IL-1β	F: 5′-CCGACCACCACTACAGCAAGG-3′ R: 5′-GGGCAGGGAACCAGCATCTTC-3′
IL-6	F: 5′-GCCTTCGGTCCAGTTGCCTTC-3′ R: 5′-GTTCTGAAGAGGTGAGTGGCTGTC-3′
IL-8	F: 5′-ACTGAGAGTGATTGAGAGTGGAC-3′ R: 5′-AACCCTCTGCACCCAGTTTTC-3′
MMP-3	F: 5′-AGTCTTCCAATCCTACTGTTGCT-3′ R: 5′-TCCCCGTCACCTCCAATCC-3′
CCL-2	F: 5′-CAGCCAGATGCAATCAATGCC-3′ R: 5′-TGGAATCCTGAACCCACTTCT-3′
IL-10	F: 5′-TCAAGGCGCATGTGAACTCC-3′ R: 5′-GATGTCAAACTCACTCATGGCT-3′
TGF-β	F: 5′-GCCCTGGACACCAACTATTGC-3′ R: 5′-AGGCTCCAAATGTAGGGGCAG-3′
β-Actin	F: 5′-ACCCTGAAGTACCCCATCGAG-3′ R: 5′-AGCACAGCCTGGATAGCAAC-3′

qPCR, quantitative polymerase chain reaction; *IL-1β*, interleukin-1 beta; *IL-6*, interleukin-6; *IL-8*, interleukin-8; *MMP-3*, matrix metalloproteinase-3; *CCL-2*, C-C motif chemokine ligand 2; *IL-10*, interleukin-10; *TGF-β*, transforming growth factor-beta.

Western Blot Analysis

Total protein was extracted from synovial tissues and synovial fibroblasts using RIPA lysis buffer (Solarbio, Beijing) containing protease and phosphatase inhibitors (P1045, Beyotime, Shanghai, China). Proteins were separated by SDS-PAGE and then transferred onto

PVDF membranes. The membranes were blocked with 5% skim milk at room temperature for one hour, then incubated overnight at 4 °C with primary antibodies. After washing with TBST, the membranes then underwent a 1-hour incubation with the appropriate secondary antibodies (goat anti-rabbit IgG; G1213-100UL, Servicebio, China, 1:5000). Following another TBST wash, protein bands were identified using a high-sensitivity enhanced chemiluminescence (ECL) chemiluminescence reagent (BL523B, Biosharp, Guangzhou, China) and visualized with a Mini-Chemi 610 chemiluminescence imaging system (Sagecreation, Beijing, China). Protein intensities were quantified with ImageJ software (version 1.54f; National Institutes of Health, Bethesda, MD, USA).

Primary antibodies used were as follows: anti-IκBα (ab32518, Abcam, USA,1:1000), anti-p-IκBα (ab133462, Abcam, USA, 1:1000), anti-MMP-3 (ab52915, Abcam, USA, 1:1000), anti-TLR4 (GB11519-100, Servicebio, China, 1:1000), anti-P65 (8242T, CST, USA, 1:1000), anti-p-P65 (3033T, CST, USA, 1:1000), anti-HMGB1 (ab79823, Abcam, USA, 1:1000), anti-IL-25 (ab180594, Abcam, USA, 1:1000), anti-NLRP3 (19771-1-AP, Wuhan Sanying, China, 1:1000), anti-β-actin (AF7018, Affinity, USA, 1:1000).

Wound Healing Assay

RA-FLSs were seeded into 6-well plates and cultured overnight. A sterile 200 µL pipette tip was employed to create a linear scratch in the center of each well. The cells were then washed three times with PBS to eliminate detached cells. Serum-free medium containing IL-25 and/or TNF-α was then added. Images were acquired at 0 and 24 hours using an inverted fluorescence microscope, and the scratch area was determined using ImageJ software.

Migration and Invasion Assay

For migration assays, treated RA-FLSs were resuspended in serum-free DMEM at a density of 2×10^4 cells per well and seeded into the upper chamber of a Transwell insert (3422, Corning, NY, USA). The lower chamber was filled with DMEM containing 20% FBS. Cells were cultivated for 24 hours at 37 °C.

For invasion assays, the upper chamber was precoated with Matrigel (diluted 1:19 in buffer) and allowed to solidify overnight at 4 °C before cell seeding. After incubation, the inserts were removed, washed twice with PBS, and stained with 1% crystal violet in methanol for 30 minutes at room temperature. After PBS washing and air-drying, cells that had migrated or invaded to the lower surface were counted manually using an inverted fluorescence microscope.

Micro-Computed Tomography

Mouse ankle joints preserved in 4% paraformaldehyde were mounted on the scanner sample holder and stabilized with foam supports. Micro-CT scanning was conducted using a Scanco system (Zurich, Switzerland) under the following conditions: 80 kV, 500 µA, 15 µm resolution, and a 0.5 mm aluminum filter. The acquired datasets were then reconstructed to create 3D images of the joints.

Statistical Analysis

Statistical analyses were performed using GraphPad Prism 10.0 (GraphPad Software Inc., San Diego, CA, USA) and SPSS 19.0 (SPSS, Chicago, IL, USA). All experiments were conducted in triplicate, and data were presented as mean $\pm$ standard error of the mean (SEM). Comparison between the two groups was performed with independent samples *t*-tests. In contrast, comparisons among three or more groups were conducted using one-way ANOVA followed by Tukey's HSD post hoc test. Spearman correlation analysis was used to assess associations. A *p*-value of less than 0.05 was considered statistically significant.

Results

Increased IL-25 and IL-6 Levels in Joint Fluid of RA Patients and Their Association With Disease Activity

IL-25 and IL-6 protein levels were significantly elevated in RA joint fluid compared to controls (Fig. 1a,b, $p < 0.01$). When stratified by disease activity, no substantial difference was observed in IL-25 and IL-6 levels between the low-activity (LRA) and high-activity (HRA) RA groups (Fig. 1c,d). Correlation analysis revealed that IL-6 levels were positively associated with Erythrocyte Sedimentation Rate (ESR) ($p < 0.05$), whereas IL-25 levels showed no significant correlation with inflammation markers (Fig. 1e–j).

Overexpression of IL-25 in Synovial Tissue and Synovial Fibroblasts

To determine IL-25 expression in RA and controls, synovial tissues were collected from 3 RA and 3 OA patients, and FLSs were then isolated. IL-25 expression in tissues and cells was assessed by WB, IHC, and H&E staining. H&E staining showed significant synovial lining hyperplasia, disorganized synovial cell arrangement, and inflammatory cell infiltration in RA compared to OA (Fig. 2a). IHC staining (Fig. 2b,g) revealed that IL-25 was primarily localized in the cytoplasm, with significant upregulation in RA synovial tissue compared to OA ($p < 0.001$). Consistently, WB analysis confirmed significantly elevated IL-25 expression in both RA synovial tissue ($p < 0.05$) and primary FLSs ($p < 0.001$) compared to OA (Fig. 2c–f).

IL-25 Inhibits TNF-α-Induced Inflammatory Mediator Production in RA-FLSs

After treatment, FLSs were observed migrating from the edges of the tissue under an inverted microscope, predominantly showing a spindle-shaped morphology with centrally located nuclei and a vortic-like growth pattern.

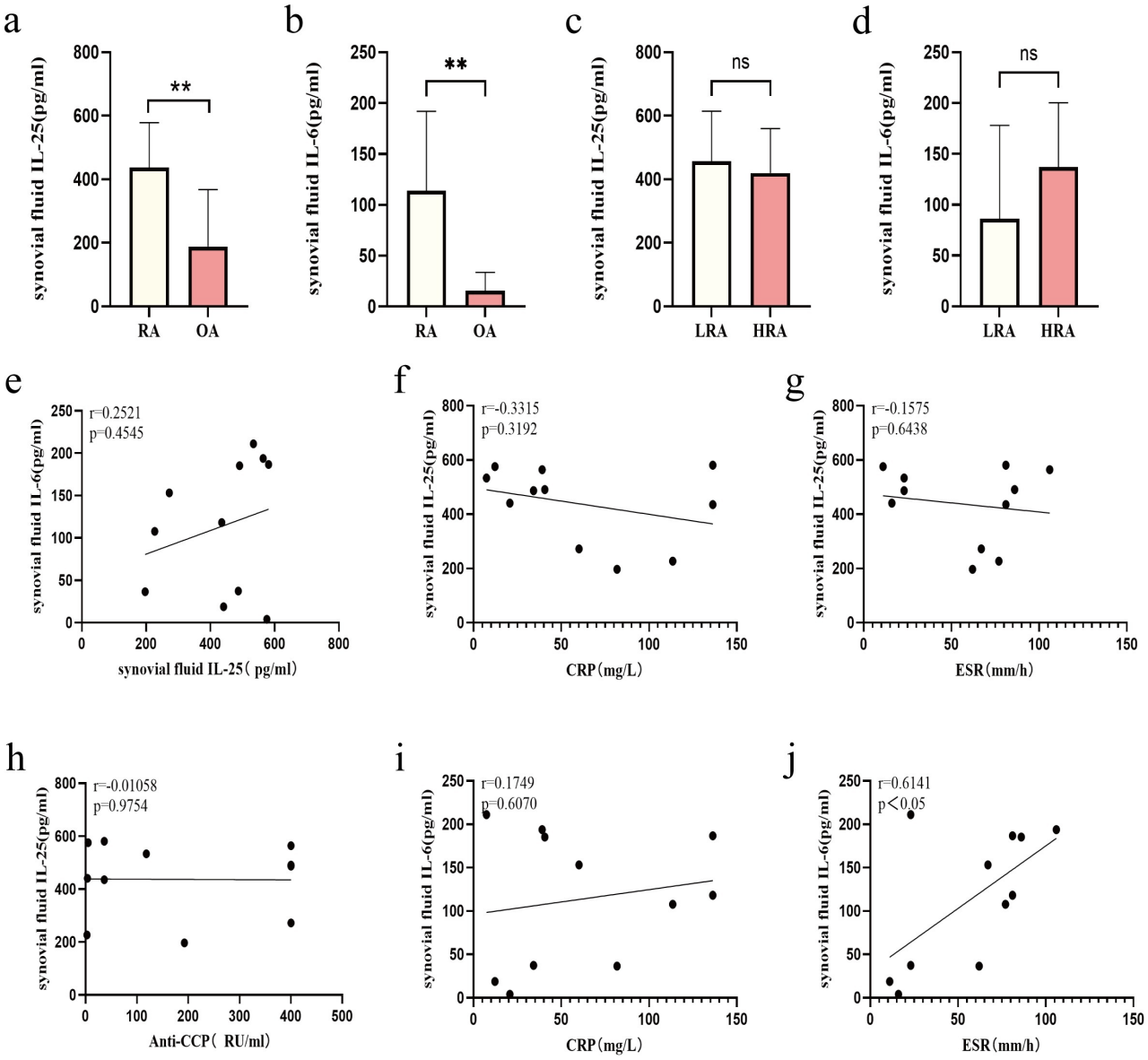

Fig. 1. The concentrations and interrelationship of interleukin-25 (IL-25) and IL-6 in rheumatoid arthritis (RA) patients. (a,b) When compared to patients with osteoarthritis (OA) (n = 6), RA patients (n = 11) showed a substantial increase in IL-25 and IL-6 levels. (c,d) No significant difference was observed in IL-25 and IL-6 levels between low-activity RA patients (LRA) (n = 5) and high-activity RA patients (HRA) (n = 6). (e–j) IL-6 in joint effusion exhibited a positive correlation with Erythrocyte Sedimentation Rate (ESR); however, no substantial association was observed between IL-25 levels and disease activity. Statistical significance is expressed as $^{**}p < 0.01$, and "ns" indicates no significant difference.

Occasionally, pseudopodia-like macrophages were also identified. The cells maintained a stable growth state when cultured and passaged to the third generation. Under a fluorescence microscope, synovial fibroblasts showed green-stained cytoplasm with Vimentin and blue-stained nuclei with DAPI, confirming a purity of over 99% after image merging (Fig. 3a–d).

Activated RA-FLSs secrete inflammatory mediators and MMPs, with TNF-α stimulation further increasing inflammation, synovitis, and bone destruction. To investigate the role of IL-25 in regulating MMPs and inflammatory mediators in RA-FLSs, cells were treated with varying concentrations of IL-25. It was found that 10 ng/mL of IL-25 increased inflammatory responses, whereas 100 ng/mL substantially suppressed inflammation ($p < 0.05$, $p < 0.0001$, Fig. 3e–g). Based on these findings, further experiments were conducted using 100 ng/mL of IL-25. RA-FLSs were stimulated with TNF-α and/or IL-25 for 24 hours, and WB analysis assessed levels of the inflammatory protein HMGB1 and the bone erosion-related MMP-3.

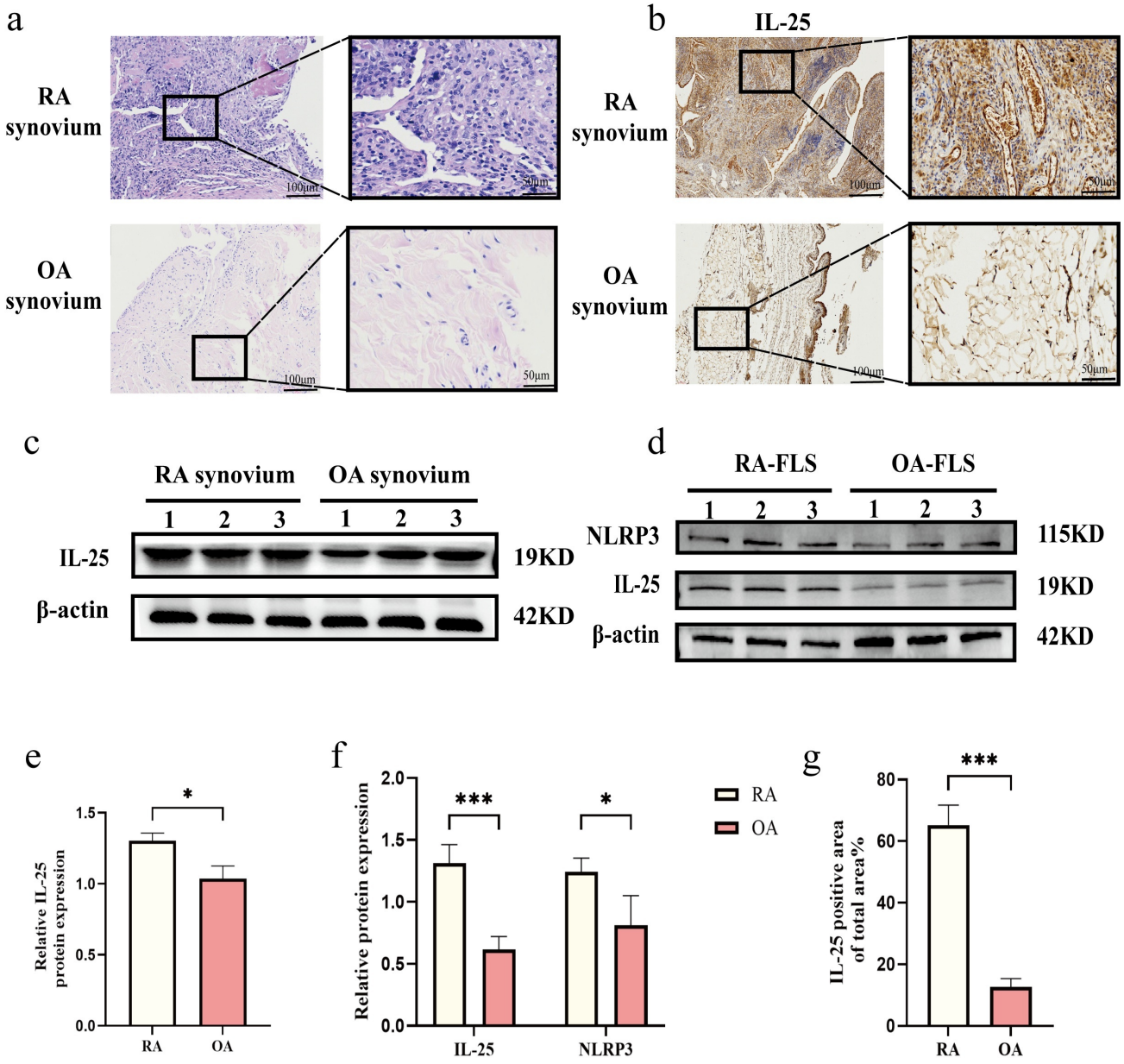

Fig. 2. Increased IL-25 expression in the synovial tissue of RA patients. (a) Representative images from H&E staining show IL-25 in the synovial tissues of RA and OA patients (n = 3). (b,g) Immunohistochemical staining (IHC) Paraffin-embedded human knee joint tissue samples were deparaffinized, followed by antigen retrieval using citrate buffer. Subsequently, the sections were subjected to DAB staining and counterstained with hematoxylin. After dehydration through a graded alcohol series, the samples were resin-mounted and examined using a fluorescence microscope (Olympus, Japan). staining shows IL-25 in the synovial tissues of RA and OA (n = 3). (c,e) Western blot analysis was employed to measure IL-25 protein levels in synovial tissues of RA (n = 3) and OA (n = 3) patients. (d,f) The protein levels of IL-25 and NLRP3 in primary fibroblast-like synoviocytes from RA (n = 3) and OA (n = 3) patients (Western blot analysis). β-actin served as a reference gene. Data obtained from three independent experiments were expressed as mean ± SEM. *$p <$ 0.05, ***$p < 0.001$.

Furthermore, Pretreatment with 100 ng/mL IL-25 significantly downregulated HMGB1 and MMP-3 protein expression compared to stimulation by 50 ng/mL TNF-α alone ($p < 0.05$, $p < 0.01$, Fig. 3h–j). Additionally, qRT-PCR was used to assess mRNA expression of inflammatory factors. mRNA levels of *IL-1*β, *IL-6*, *IL-8*, and the chemokine CCL-2 were significantly downregulated in RA-FLSs pretreated with 100 ng/mL IL-25 ($p < 0.05$, $p < 0.0001$, Fig. 3k–n). However, no significant differences were found in IL-10 or TFG-β expression between the groups ($p > 0.05$, Fig. 3o,p), nor in IL-17RA and IL-17RB ($p > 0.05$, Fig. 3q,r). Moreover, IL-6 levels in cell su-

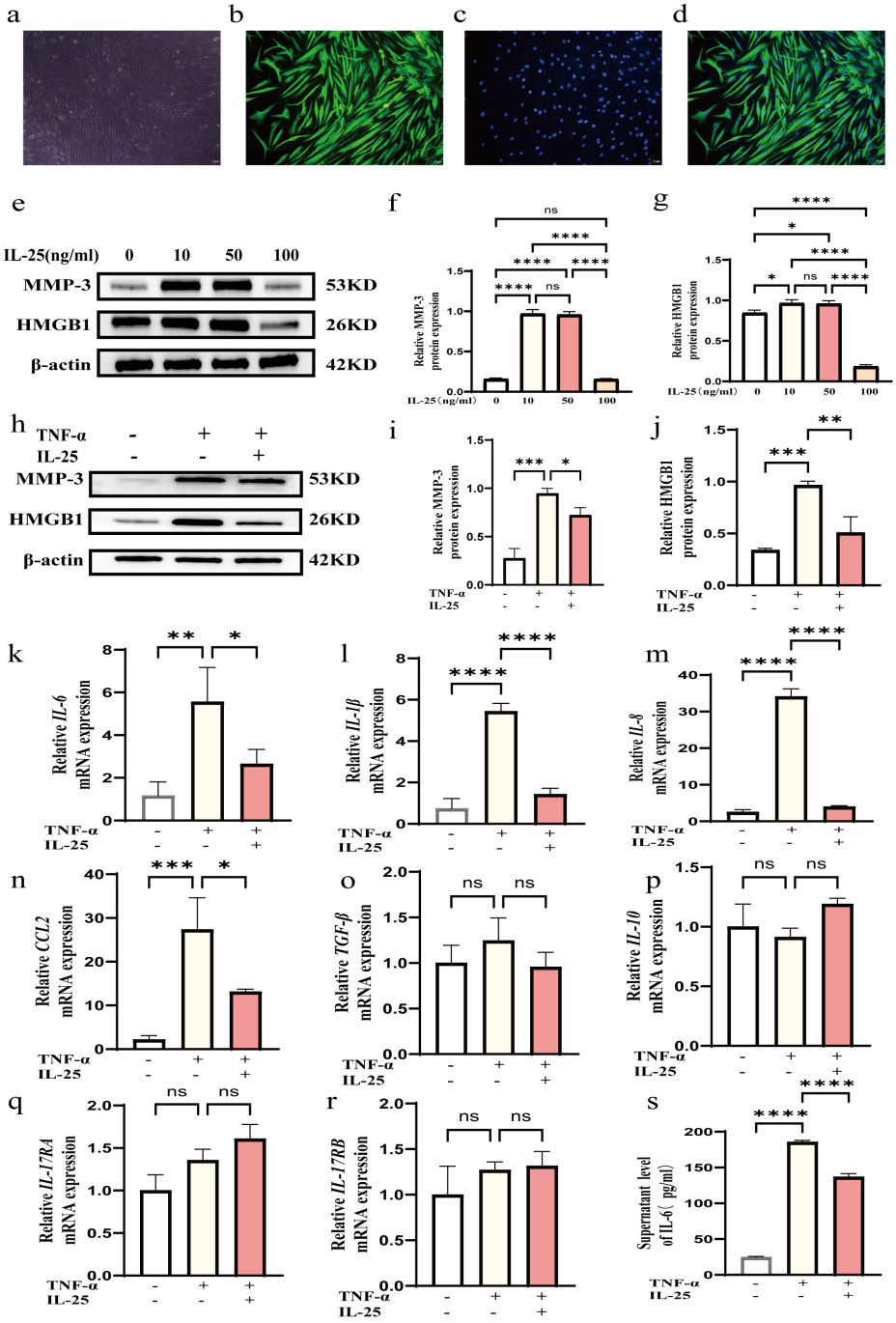

Fig. 3. IL-25 reduces tumor necrosis factor-α (TNF-α)-induced inflammation in RA-FLSs. (a–d) Morphological identification and immunofluorescence staining of synovial fibroblasts (a: Under the microscope, the third-generation RA-FLS are mostly spindle-shaped, with the nucleus located in the center. b: Under the fluorescence microscope, the RA-FLS Vimentin protein shows green fluorescence; c: All the cell nucler in the field of view were stained blue by DAPI dye. d: Synthesize figures b and c, and the purity of RA-FLS is greater than 99%). (e–g) Impact of different concentrations of IL-25 on RA-FLS. (h–j) Protein levels of MMP-3 and high mobility group box-1 protein (HMGB1) in RA-FLSs stimulated with TNF-α (50 ng/mL) and IL-25 (100 ng/mL) for 24 hours (Western blot analysis). (k–n) mRNA expression levels of *IL-6*, *IL-1*β, *IL-8*, and *CCL-2* in RA-FLSs treated with TNF-α (50 ng/mL) and IL-25 (100 ng/mL) for 24 hours (qRT-PCR). (o–r) mRNA expression levels of transforming growth factor-beta (*TGF-*β), *IL-10*, *IL-17RA*, and *IL-17RB* in RA-FLSs received TNF-α (50 ng/mL) and IL-25 (100 ng/mL) treatment for 24 hours (qRT-PCR). (s) IL-6 levels in the supernatant from different groups, as assessed using enzyme-linked immunosorbent assay (ELISA). β-Actin was employed as a reference gene. Data were expressed as mean $\pm$ SEM from three independent experiments. Statistical significance is denoted as $^{*}p < 0.05$, $^{**}p < 0.01$, $^{***}p < 0.001$, $^{****}p < 0.0001$, and "ns" indicates no significant difference.

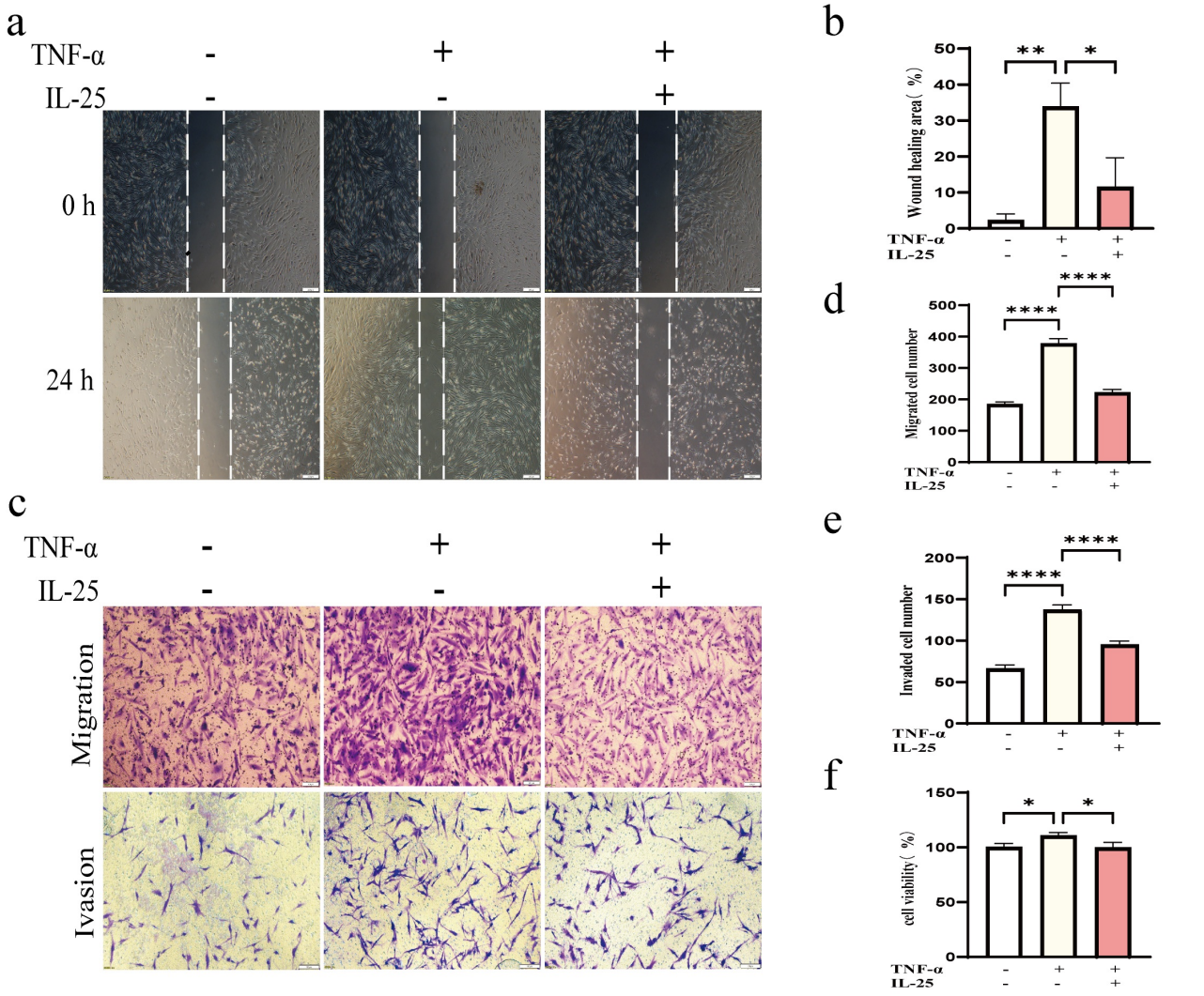

Fig. 4. IL-25 reduces TNF-α-induced migration and invasion of RA-FLSs. (a,b) Representative images from the wound healing assay, indicating the wound healing rates across various groups after 24 hours, with a scale bar of 200 µm. (c–e) Migratory and invading capability of cells across different groups assessed by the Transwell assay, scale bar of 200 µm. (f) The Cell Counting Kit-8 (CCK-8) assay is used to examine cell viability. Data were expressed as mean ± SEM from three independent experiments. Statistical significance is denoted as *$p < 0.05$, **$p < 0.01$, ****$p < 0.0001$.

pernatants increased after TNF-α stimulation but were significantly decreased when cells were pretreated with IL-25 before TNF-α induction ($p < 0.0001$, Fig. 3s).

IL-25 Inhibits TNF-α-Induced Invasion, Migration, and Proliferation of RA-FLSs In Vitro

Furthermore, we investigated the impact of IL-25 on the migration, invasion, and proliferation of RA-FLSs. Wound healing assay (Fig. 4a,b) showed that 50 ng/mL TNF-α significantly enhanced RA-FLSs migration ($p < 0.01$). However, pretreatment with 100 ng/mL IL-25 for 4 hours before TNF-α induction significantly attenuated this enhanced migration ($p < 0.05$). These results were further supported by Transwell assays ($p < 0.0001$), which revealed consistent results (Fig. 4c–e).

Similarly, the CCK-8 assays showed that TNF-α (50 ng/mL) significantly enhanced RA-FLSs proliferation, but pretreatment with 100 ng/mL IL-25 before TNF-α stimulation substantially suppressed this effect ($p < 0.05$, Fig. 4f).

Collectively, these results indicate that IL-25 attenuates TNF-α-mediated migration, invasion, and proliferation of RA-FLSs, likely by inhibiting inflammatory pathways.

IL-25 Reduces TNF-α-Induced Expression of NLRP3, TLR4, and NF-κB

To investigate the mechanism by which IL-25 modulates inflammation in RA, we focused on the TLR4/NF-κB/NLRP3 signaling pathway, which plays a crucial role in inflammation. The NF-κB pathway is known to contribute significantly to RA pathogenesis through modulation of

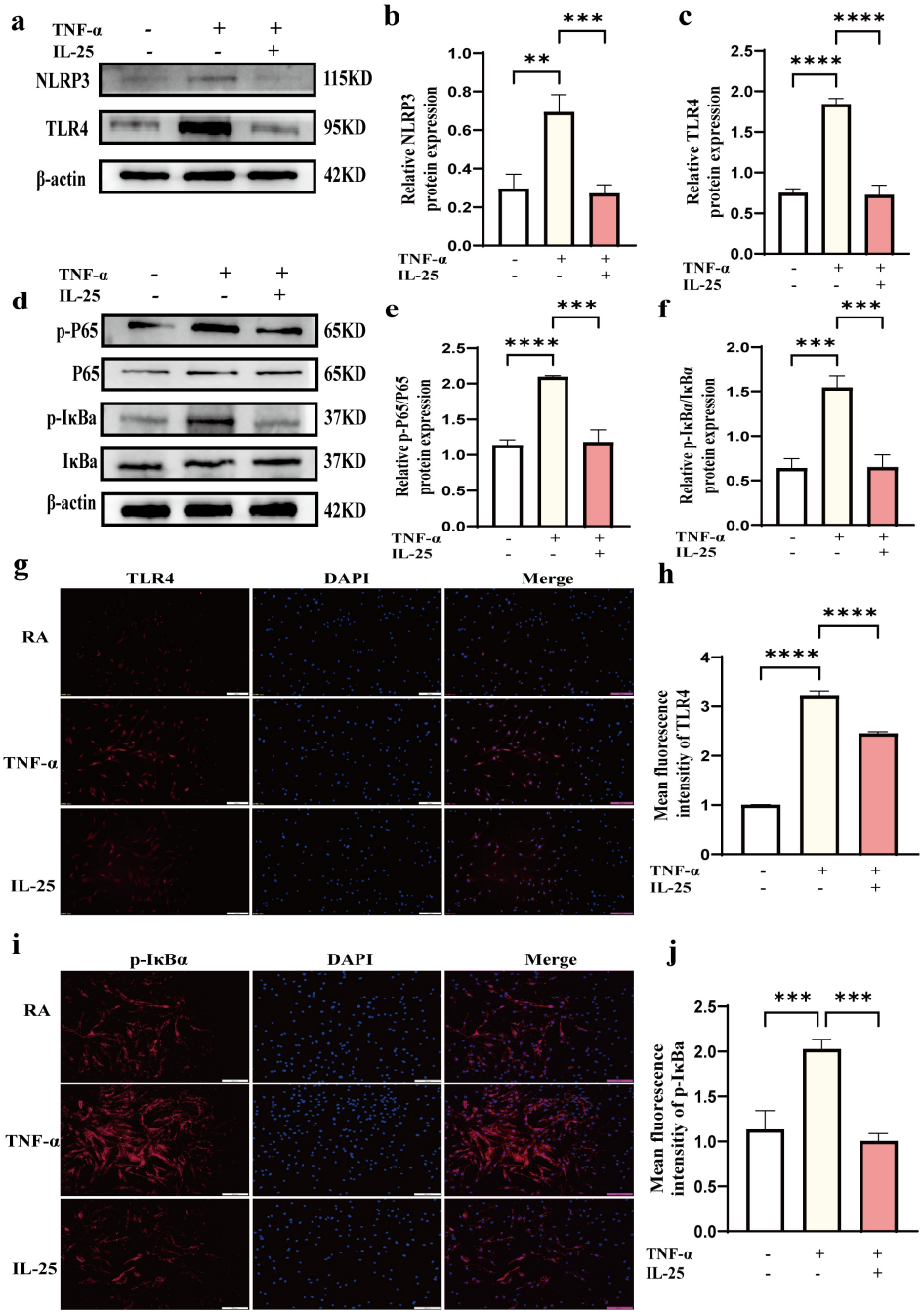

Fig. 5. IL-25 alleviates inflammation in RA-FLSs through the TLR4/NF-κB/NLRP3 signaling pathway. (a–c) RA-FLS protein levels of TLR4 and NLRP3 following treatment with various concentrations of TNF-α and IL-25 for 24 hours (Western blot analysis). (d–f) The protein levels of P65, p-P65, IκBα, and p-IκBα in RA-FLSs under the same treatment conditions (Western blot analysis). (g–j) Representative immunofluorescence staining images of TLR4 and p-IκBα in RA-FLSs treated with TNF-α and IL-25 for 24 hours, with a scale bar of 500 µm. β-Actin was employed as a reference gene. Data were presented as mean ± standard deviation, as determined by scanning electron microscopy from three independent experiments. Statistical significance is denoted as $^{**}p < 0.01$, $^{***}p < 0.001$, $^{****}p < 0.0001$.

pro-inflammatory cytokine production [22,23]. WB analysis showed that IL-25 pretreatment significantly reduced TLR4 and NLRP3 protein expression in TNF-α-stimulated RA-FLSs compared to TNF-α treatment alone ($p < 0.0001$, $p < 0.001$, Fig. 5a–c). Concurrently, IL-25 pretreatment effectively suppressed the phosphorylation levels of p65 and IκBα proteins activated by TNF-α ($p < 0.001$, Fig. 5d–f). Immunofluorescent staining further confirmed that TNF-α stimulation significantly increased the fluorescence intensity of TLR4 and p-IκBα, whereas IL-25 pretreatment at-

tenuated these responses ($p < 0.0001$, $p < 0.001$, Fig. 5g–j). The findings demonstrate that IL-25 inhibits activation of the TLR4/NF-κB/NLRP3 pathway.

IL-25 Negatively Regulates Joint Inflammation and Bone Erosion in the CIA Model

In vitro analyses revealed that high concentrations of IL-25 inhibit TNF-α-mediated inflammation through the TLR4/NF-κB/NLRP3 signaling pathway, attenuate RA-FLSs proliferation and erosive capacity, and reduce the release of inflammatory cytokines and bone destruction. The primary aim of the *in vivo* study was to assess the therapeutic potential of IL-25 in the RA mouse model, thereby providing a theoretical basis for future clinical applications.

Recombinant murine IL-25 was administered in the CIA mouse model. After successful establishment (day 21), mice received intraperitoneal injections of either PBS or recombinant murine IL-25 (0.05 µg/kg/day) (Fig. 6a). Hind paw swelling in the CIA group was more pronounced compared to the IL-25-treated group (Fig. 6b). Furthermore, body weight loss was substantially higher in the CIA group compared to the IL-25 group from day 1 post-booster immunization until the end of the study ($p < 0.05$, Fig. 6c). Similarly, arthritis index scores were significantly greater in the CIA model than in the IL-25 treatment groups ($p < 0.05$, Fig. 6d).

Histological assessment using H&E and safranin O-fast green staining of knee joints at the study endpoint showed that IL-25 intervention alleviated cartilage damage and synovial inflammation in CIA mice (Fig. 6e). Consistently, qualitative observation of Micro-CT scans demonstrated that exogenous IL-25 administration mitigated bone erosion and destruction in the CIA model (Fig. 6f). Furthermore, enzyme-linked immunosorbent assay revealed substantially reduced expression of TNF-α, IL-6, and IL-17 in the peripheral blood of the IL-25-treated group compared to the CIA model group ($p < 0.0001$, Fig. 6g). These findings further support the anti-inflammatory role of IL-25 in RA. These results demonstrate that IL-25 effectively alleviates synovial inflammation and reduces joint damage in collagen-induced arthritic mice.

Discussion

Rheumatoid arthritis is a chronic inflammatory condition that leads to joint deformities and systemic manifestations [24]. Due to its complex pathogenesis, the underlying mechanisms of RA pathogenesis remain incompletely understood, leading to poor treatment outcomes [25]. However, persistent inflammation is recognized as a key pathogenic driver [26]. The previous study has identified that pro-inflammatory cytokines TNF-α, IL-1β, and IL-6 promote the expression of various catabolic mediators, thereby disrupting joint integrity. These cytokines stimulate MMP production, increase neutrophil and macrophage infiltration, and ultimately amplify the inflammatory response [27]. Particularly, TNF-α upregulates MMP-1, MMP-3, IL-1β, IL-6, and IL-8, thereby enhancing inflammation and extracellular matrix (ECM) degradation [28,29]. Through these mechanisms, chronic inflammation and ECM degradation intensify, driving the progression of persistent RA.

The previous study has reported that the expression of IL-25 in the serum of RA patients was significantly increased, which leads to bone erosion and interstitial lung lesions [18], suggesting a potential pro-inflammatory effect. However, further experiments revealed that at higher concentrations, IL-25 decreases the levels of other pro-inflammatory factors in synovial fibroblasts, indicating a context-dependent regulatory function.

In this study, we established a TNF-α-induced high-inflammatory state in RA-FLSs to mimic the RA inflammatory process. Representative inflammatory factors were examined to explore the role of IL-25. We observed that TNF-α treatment significantly increased the expression of IL-1β, IL-6, MMP-3, and HMGB1. However, exposure to high-concentration IL-25 (100 ng/mL) substantially reduced TNF-α-induced inflammation and downregulated these mediators, indicating that IL-25 can attenuate TNF-α-induced inflammatory responses in RA-FLSs *in vitro*. To further validate these outcomes, we established a CIA mouse model to observe the effects of IL-25 on joint inflammation and damage *in vivo*. IL-25 treatment alleviated collagen-induced joint damage and exerted a protective effect by reducing the release of pro-inflammatory mediators such as IL-1β, IL-6, and IL-17, thereby preventing enhanced inflammatory cascades. These findings are consistent with previous results [20].

IL-25 has been reported to exert suppressive effects across a range of inflammatory immune disorders. *In vitro* studies demonstrated that IL-25 inhibits the production of TNF, IFNγ, and IL-17A in $CD4^+$ T cells from IBD patients, thereby suppressing Th1 and Th17 differentiation [30]. In systemic lupus erythematosus (SLE), IL-25 expression is dysregulated; elevated IL-25 levels have been shown to suppress inflammatory responses in SLE mouse models by reducing pro-inflammatory cytokines, thereby participating in lupus pathogenesis [31]. In RA, previous research evidence has indicated that IL-25 pretreatment of RA-FLSs downregulates STAT3, p38, and IκB-α phosphorylation induced by IL-22 stimulation [21]. Consistent with these observations, our study found significantly increased IL-25 expression in RA patient tissues and synovial fluid compared to controls, as well as elevated IL-25 levels in CIA mouse tissues compared to controls.

Given the anti-inflammatory effects of IL-25, we hypothesized that IL-25 may play a crucial role in suppressing inflammation associated with RA. High mobility group box-1 protein (HMGB1) serves as an alarmin; once released from the cell, HMGB1 binds to Toll-like receptors

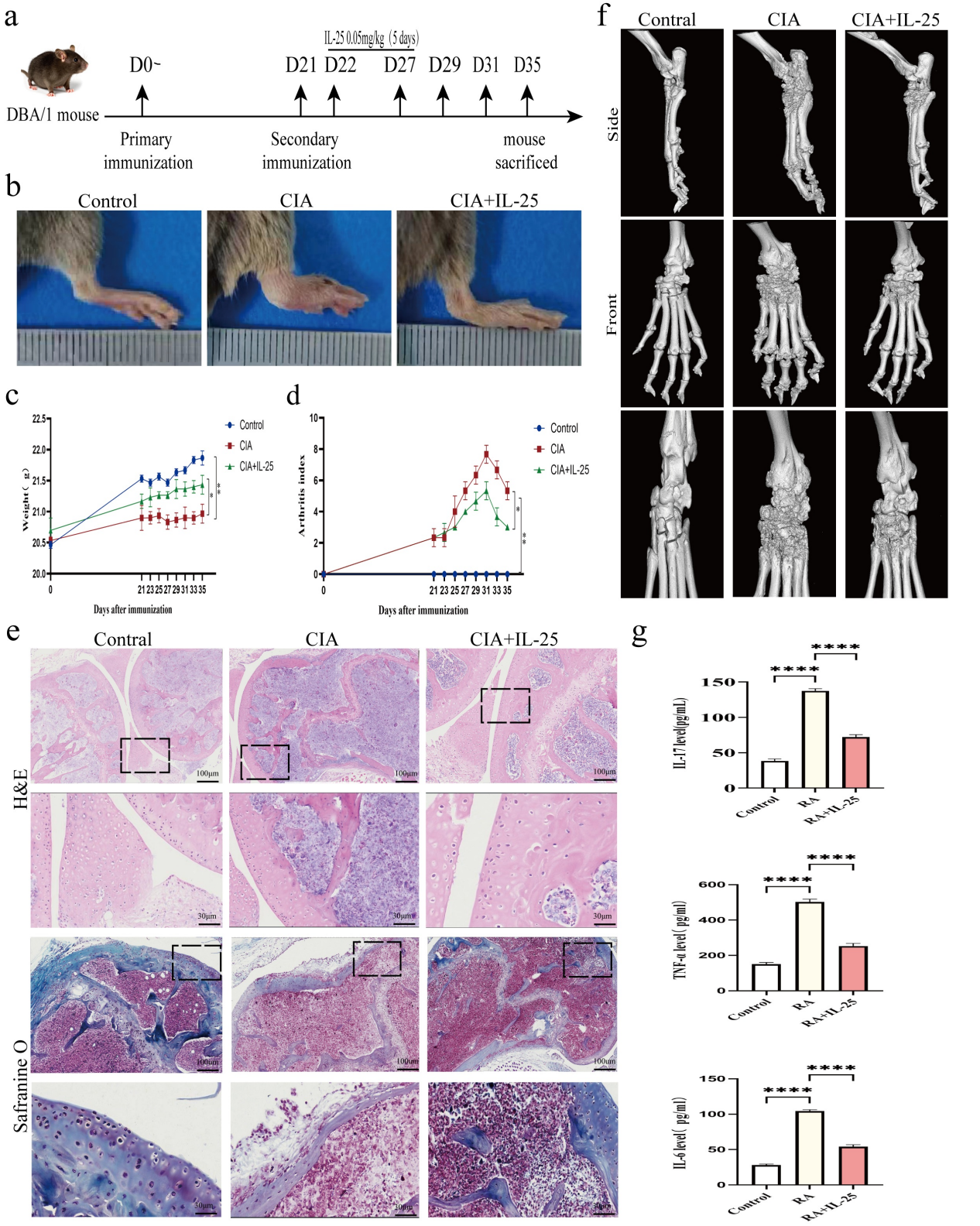

Fig. 6. IL-25 is instrumental in alleviating joint inflammation and mitigating bone damage in collagen-induced arthritis mice. (a) The schedule for the animal experiments details the progression and treatment of collagen-induced arthritis (CIA). (b) Representative images of mice's paws. (c,d) The influence of IL-25 on the weight and arthritis index in mice. (e) Histological findings (n = 3 rats). Representative images of mouse knee joints stained with HE and safranin O-fast green. (f) Micro-CT images of mouse ankle joints. (g) Plasma levels of tumor necrosis factor-α, IL-6, and IL-17 proteins in different groups were assessed through enzyme-linked immunosorbent assay. Data were presented as mean $\pm$ SEM. *$p < 0.05$, **$p < 0.01$, ****$p < 0.0001$.

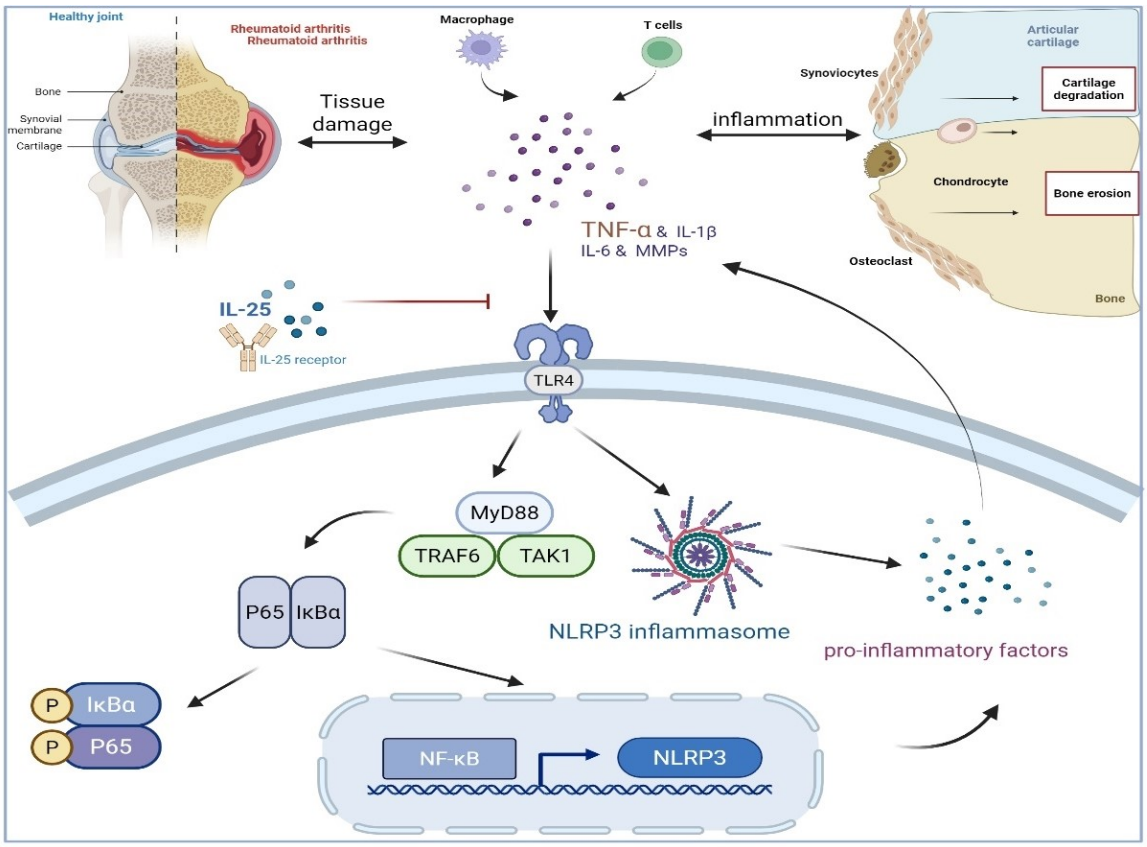

Fig. 7. Mechanistic illustration of IL-25 inhibiting RA-FLSs activity. In RA, the persistent presence of inflammatory factors alters the synovial microenvironment, facilitating the stimulation of FLS through complex inflammatory interactions. IL-25 mitigates inflammation by suppressing the secretion of pro-inflammatory cytokines and inhibiting activation of the NF-κB signaling pathway. The figure was created with BioRender (https://www.biorender.com/).

(TLRs), including TLR2 and TLR4, converting them into a potent pro-inflammatory mediator. This interaction is significantly involved in the initiation and progression of autoimmune diseases [32]. Notably, inhibiting HMGB1 and TLRs signaling suppresses inflammation responses in animal models [33].

RA is characterized by persistent inflammation accompanied by bone destruction and erosion. The TLR/NF-κB/NLRP3 signaling pathway, consisting of TLR activation, NF-κB signaling, and NLRP3 inflammasome priming, plays a crucial role in orchestrating inflammatory responses across various organs. Both inflammation and NF-κB pathway activation are central components of RA progression. The transcriptional activity of NF-κB p65 is regulated through multiple mechanisms, including post-translational modifications (such as phosphorylation and acetylation) and interactions with other transcription factors, cofactors, or co-inhibitors. During inflammation, NF-κB p65 modulates the expression of key cytokines such as TNF-α and IL-1β [34]. Prior research has indicated that activation of NF-κB signaling promotes inflammatory cytokine expression and ECM degradation, thereby exacerbating RA progression. Whereas inhibiting NF-κB signaling can alleviate RA progression [35]. TLRs are transmembrane pattern recognition receptors that regulate inflammatory cytokine expression by activating NF-κB and MAPK pathways [36]. The NLRP3 inflammasome complex, composed of NLRP3, apoptosis-related speck-like protein (ASC) and caspase-1, functions as a key regulator of innate immune responses and inflammation [37].

In our study, TNF-α (50 ng/mL) significantly activated the NF-κB pathway, as evidenced by elevated p-P65 and p-IκBα levels. IL-25 (100 ng/mL) treatment significantly reduced the expression of p-IκBα, p-P65, TLR4, and NLRP3 protein, accompanied by a reduction in the secretion of IL-1β, IL-6, and MMP-3. Since aberrant activation of RA-FLSs is a key driver of joint destruction, these results confirm that IL-25 suppresses the inflammatory phenotype and activation of RA-FLSs by regulating the TLR4/NF-κB/NLRP3 signaling pathway. High concentrations of IL-25 were found to reduce TNF-α-mediated pro-inflammatory cytokine release, thereby diminishing RA-FLSs migration and invasion (Fig. 7). The TLR4/NF-κB/NLRP3 signaling pathway, as a classic regulator of inflammation, significantly contributes to this process. By inhibiting the “TLR4 to NF-κB to NLRP3” signaling axis,

IL-25 exerts a sequential inhibitory effect, disrupting the positive feedback loop that drives chronic inflammation in RA.

In summary, this study confirmed elevated IL-25 expression in synovial fluid and tissues of RA patients. *In vitro*, IL-25 was found to attenuate the proliferation and migration of RA-FLSs by restraining inflammation and modulating the TLR4/NF-κB/NLRP3 pathway. Finally, *in vivo* experiments demonstrated that IL-25 exerted a protective effect against cartilage erosion in the CIA mouse model. These results provide novel insights into the role of IL-25 in RA and underscore its potential as a molecular target for future therapeutic approaches.

Despite its promising outcomes, this study still has some limitations. First, due to the challenges in collecting sufficient joint fluid, the sample size for detection was relatively small, and there was no obvious correlation between IL-25 and inflammatory indicators. Hence, future studies should expand the sample size to validate these results. Second, as this was a preliminary exploratory investigation, the small number of animals limited statistical power, which should be addressed in future research. Finally, while this study provided initial evidence of IL-25 intervention on the basic phenotype of RA disease models and preliminarily explored NF-κB pathway molecules; however, more comprehensive mechanistic studies, such as inhibitor-based validation experiments, were not conducted. Additionally, whether IL-25 indirectly affects the function of FLSs by regulating other cell types, such as macrophages, remains unknown. Future research incorporating single-cell sequencing could help identify the cell-specific effects of IL-25 and further evaluate its therapeutic potential.

Conclusion

This study confirmed that elevated IL-25 alleviates RA-FLSs proliferation and joint destruction by regulating inflammatory responses and inhibiting disease progression. Our findings also suggest that IL-25 may modulate the phosphorylation of p65 through the TLR4/NF-κB/NLRP3 pathway. These findings indicate a potential bidirectional role of IL-25 in RA. Further comprehensive studies are warranted to elucidate additional mechanisms of IL-25 and to better investigate its interactions with other inflammatory factors in RA.

Availability of Data and Materials

The datasets used and/or analyzed during the current study are available from the corresponding author upon reasonable request.

Author Contributions

Conceptualization, JYL and HLS; methodology, JXZ and HYL; software, JYL; validation, JYL and JYH; formal analysis, JYL; investigation, JYL; resources, JYL and HYL; data curation, JYL and CHL; writing—original draft preparation, all authors; writing—review and critical revision, all authors; visualization, JYH; supervision, HYL; project administration, CHL; funding acquisition, JYL. All authors have read and approved the final manuscript. All authors have participated sufficiently in the work and agreed to be accountable for all aspects of the work.

Ethics Approval and Consent to Participate

The study protocol received approval from the ethics committee of The Second Hospital & Clinical Medical School, Lanzhou University (protocol No: 2025A-717). Written informed consent was obtained from all participants. All procedures involving human participants were conducted in accordance with the Declaration of Helsinki. All animal experiments were approved by the Ethics Committee of The Second Hospital & Clinical Medical School, Lanzhou University (Ethics Approval No: D2025-473) and performed in accordance with institutional guidelines and the National Institutes of Health Guide for the Care and Use of Laboratory Animals. All efforts were made to minimize animal suffering.

Acknowledgment

Not applicable.

Funding

This work was funded by the Youth Science and Technology Fund of Gansu Province (Grant No.21JR11RA117); Lanzhou Science and Technology Bureau Project (Grant No.2023-2-3); Gansu Provincial Health Commission Project (Grant No.GSWSKY2024-01); Gansu Provincial Bureau of Traditional Chinese Medicine Project (Grant No.GZKZ-2024-27); Lanzhou Science and Technology Bureau Project (Grant No.2024-3-77).

Conflict of Interest

The authors declare no conflict of interest. Fig. 7 was created using BioRender. The authors have no financial or personal relationship with BioRender, and the use of this tool does not imply any endorsement.

References

[1] Nygaard G, Firestein GS. Restoring synovial homeostasis in rheumatoid arthritis by targeting fibroblast-like synoviocytes. Nature Reviews. Rheumatology. 2020; 16: 316–333. https://doi.org/10.1038/s41584-020-0413-5.

[2] Jang S, Kwon EJ, Lee JJ. Rheumatoid Arthritis: Pathogenic Roles of Diverse Immune Cells. International Journal of Molecular Sciences. 2022; 23: 905. https://doi.org/10.3390/ijms23020905.

[3] Komatsu N, Takayanagi H. Mechanisms of joint destruction in rheumatoid arthritis - immune cell-fibroblast-bone interactions. Nature Reviews. Rheumatology. 2022; 18: 415–429. https://doi.org/10.1038/s41584-022-00793-5.

[4] Tsaltskan V, Firestein GS. Targeting fibroblast-like synoviocytes in rheumatoid arthritis. Current Opinion in Pharmacology. 2022; 67: 102304. https://doi.org/10.1016/j.coph.2022.102304.

[5] Gu SL, Liu XS, Xu ZS, Li LL, Wu XJ, Li FL, *et al*. Eupalinolide B alleviates rheumatoid arthritis through the promotion of apoptosis and autophagy via regulating the AMPK/mTOR/ULK-1 signaling axis. International Immunopharmacology. 2025; 148: 114179. https://doi.org/10.1016/j.intimp.2025.114179.

[6] Jeong YJ, Park SA, Park YH, Kim LK, Lee HR, Kim HJ, *et al*. Anti-inflammatory effect of the combined treatment of LMT-28 and kaempferol in a collagen-induced arthritis mouse model. PloS One. 2024; 19: e0302119. https://doi.org/10.1371/journal.pone.0302119.

[7] Luo Y, Lei Y, Guo X, Zhu D, Zhang H, Guo Z, *et al*. CX-4945 inhibits fibroblast-like synoviocytes functions through the CK2-p53 axis to reduce rheumatoid arthritis disease severity. International Immunopharmacology. 2023; 119: 110163. https://doi.org/10.1016/j.intimp.2023.110163.

[8] He Q, Jia L, Wang X, Feng D, Mao T. Knockdown of BUB1 inhibits tumor necrosis factor-α-induced proliferation and migration of rheumatoid arthritis synovial fibroblasts by regulating PI3K/Akt pathway. International Journal of Rheumatic Diseases. 2023; 26: 2024–2030. https://doi.org/10.1111/1756-185X.14865.

[9] Bai LL, Chen H, Zhou P, Yu J. Identification of Tumor Necrosis Factor-Alpha (TNF-α) Inhibitor in Rheumatoid Arthritis Using Network Pharmacology and Molecular Docking. Frontiers in Pharmacology. 2021; 12: 690118. https://doi.org/10.3389/fphar.2021.690118.

[10] Kim W, Kim HJ, Trinh NT, Yeon HR, Kim JH, Choi IA, *et al*. Association between nuclear factor of activated T cells C2 polymorphisms and treatment response in rheumatoid arthritis patients receiving tumor necrosis factor-alpha inhibitors. Pharmacogenetics and Genomics. 2022; 32: 10–15. https://doi.org/10.1097/FPC.0000000000000446.

[11] Huang L, Hu S, Shao M, Wu X, Zhang J, Cao G. Combined Cornus Officinalis and Paeonia Lactiflora Pall Therapy Alleviates Rheumatoid Arthritis by Regulating Synovial Apoptosis *via* AMPK-Mediated Mitochondrial Fission. Frontiers in Pharmacology. 2021; 12: 639009. https://doi.org/10.3389/fphar.2021.639009.

[12] Zhang Y, Wang JY, Wang H, Chen XY, Zhang L, Yuan Y. An alcohol extract prepared from the male flower of Eucommia ulmoides Oliv. promotes synoviocyte apoptosis and ameliorates bone destruction in rheumatoid arthritis. Chinese Medicine. 2021; 16: 113. https://doi.org/10.1186/s13020-021-00522-2.

[13] Liu Y, Shao Z, Shangguan G, Bie Q, Zhang B. Biological Properties and the Role of IL-25 in Disease Pathogenesis. Journal of Immunology Research. 2018; 2018: 6519465. https://doi.org/10.1155/2018/6519465.

[14] Deng C, Peng N, Tang Y, Yu N, Wang C, Cai X, *et al*. Roles of IL-25 in Type 2 Inflammation and Autoimmune Pathogenesis. Frontiers in Immunology. 2021; 12: 691559. https://doi.org/10.3389/fimmu.2021.691559.

[15] Saran A, Nishizaki D, Lippman SM, Kato S, Kurzrock R. Interleukin-17: A pleiotropic cytokine implicated in inflammatory, infectious, and malignant disorders. Cytokine & Growth Factor Reviews. 2025; 83: 35–44. https://doi.org/10.1016/j.cytogfr.2025.01.002.

[16] Omata Y, Frech M, Saito T, Schett G, Zaiss MM, Tanaka S. Inflammatory Arthritis and Bone Metabolism Regulated by Type 2 Innate and Adaptive Immunity. International Journal of Molecular Sciences. 2022; 23: 1104. https://doi.org/10.3390/ijms23031104.

[17] Lavocat F, Ndongo-Thiam N, Miossec P. Interleukin-25 Produced by Synoviocytes Has Anti-inflammatory Effects by Acting As a Receptor Antagonist for Interleukin-17A Function. Frontiers in Immunology. 2017; 8: 647. https://doi.org/10.3389/fimmu.2017.00647.

[18] Lu J, DA M, Feng Y, Liu Y, Zhang S, Shen H. Elevated serum IL-25 levels in rheumatoid arthritis patients with bone erosion and interstitial lung disease. Xi Bao Yu Fen Zi Mian Yi Xue Za Zhi = Chinese Journal of Cellular and Molecular Immunology. 2017; 33: 1118–1122.

[19] Brand DD, Latham KA, Rosloniec EF. Collagen-induced arthritis. Nature Protocols. 2007; 2: 1269–1275. https://doi.org/10.1038/nprot.2007.173.

[20] Liu D, Cao T, Wang N, Liu C, Ma N, Tu R, *et al*. IL-25 attenuates rheumatoid arthritis through suppression of Th17 immune responses in an IL-13-dependent manner. Scientific Reports. 2016; 6: 36002. https://doi.org/10.1038/srep36002.

[21] Min HK, Won JY, Kim BM, Lee KA, Lee SJ, Lee SH, *et al*. Interleukin (IL)-25 suppresses IL-22-induced osteoclastogenesis in rheumatoid arthritis via STAT3 and p38 MAPK/IκBα pathway. Arthritis Research & Therapy. 2020; 22: 222. https://doi.org/10.1186/s13075-020-02315-8.

[22] Meng X, Zhang X, Su X, Liu X, Ren K, Ning C, *et al*. Daphnes Cortex and its licorice-processed products suppress inflammation via the TLR4/NF-κB/NLRP3 signaling pathway and regulation of the metabolic profile in the treatment of rheumatoid arthritis. Journal of Ethnopharmacology. 2022; 283: 114657. https://doi.org/10.1016/j.jep.2021.114657.

[23] Niu X, Song H, Xiao X, Yang Y, Huang Q, Yu J, *et al*. Tectoridin ameliorates proliferation and inflammation in TNF-α-induced HFLS-RA cells via suppressing the TLR4/NLRP3/NF-κB signaling pathway. Tissue & Cell. 2022; 77: 101826. https://doi.org/10.1016/j.tice.2022.101826.

[24] Guo Q, Wang Y, Xu D, Nossent J, Pavlos NJ, Xu J. Rheumatoid arthritis: pathological mechanisms and modern pharmacologic therapies. Bone Research. 2018; 6: 15. https://doi.org/10.1038/s41413-018-0016-9.

[25] Radu AF, Bungau SG. Management of Rheumatoid Arthritis: An Overview. Cells. 2021; 10: 2857. https://doi.org/10.3390/cells10112857.

[26] D'Orazio A, Cirillo AL, Greco G, Di Ruscio E, Latorre M, Pisani F, *et al*. Pathogenesis of rheumatoid arthritis: one year in review 2024. Clinical and Experimental Rheumatology. 2024; 42: 1707–1713. https://doi.org/10.55563/clinexprheumatol/0307ed.

[27] Xiang Y, Zhang M, Jiang D, Su Q, Shi J. The role of inflammation in autoimmune disease: a therapeutic target. Frontiers in Immunology. 2023; 14: 1267091. https://doi.org/10.3389/fimmu.2023.1267091.

[28] Nam JH, Lee JH, Choi HJ, Choi SY, Noh KE, Jung NC, *et al*. TNF-α Induces Mitophagy in Rheumatoid Arthritis Synovial Fibroblasts, and Mitophagy Inhibition Alleviates Synovitis in Collagen Antibody-Induced Arthritis. International Journal of Molecular Sciences. 2022; 23: 5650. https://doi.org/10.3390/ijms23105650.

[29] Liao H, Zheng J, Lu J, Shen HL. NF-κB Signaling Pathway in Rheumatoid Arthritis: Mechanisms and Therapeutic Potential. Molecular Neurobiology. 2025; 62: 6998–7021. https://doi.org/10.1007/s12035-024-04634-2.

[30] Caruso R, Sarra M, Stolfi C, Rizzo A, Fina D, Fantini MC, *et al*. Interleukin-25 inhibits interleukin-12 production and Th1 cell-

driven inflammation in the gut. Gastroenterology. 2009; 136: 2270–2279. https://doi.org/10.1053/j.gastro.2009.02.049.

[31] Li Y, Wang R, Liu S, Liu J, Pan W, Li F, *et al*. Interleukin-25 is upregulated in patients with systemic lupus erythematosus and ameliorates murine lupus by inhibiting inflammatory cytokine production. International Immunopharmacology. 2019; 74: 105680. https://doi.org/10.1016/j.intimp.2019.105680.

[32] Feng Z, Meng F, Huo F, Zhu Y, Qin Y, Gui Y, *et al*. Inhibition of ferroptosis rescues M2 macrophages and alleviates arthritis by suppressing the HMGB1/TLR4/STAT3 axis in M1 macrophages. Redox Biology. 2024; 75: 103255. https://doi.org/10.1016/j.redox.2024.103255.

[33] Ren W, Zhao L, Sun Y, Wang X, Shi X. HMGB1 and Toll-like receptors: potential therapeutic targets in autoimmune diseases. Molecular Medicine (Cambridge, Mass.). 2023; 29: 117. https://doi.org/10.1186/s10020-023-00717-3.

[34] Li W, Wang K, Liu Y, Wu H, He Y, Li C, *et al*. A Novel Drug Combination of Mangiferin and Cinnamic Acid Alleviates Rheumatoid Arthritis by Inhibiting TLR4/NFκB/NLRP3 Activation-Induced Pyroptosis. Frontiers in Immunology. 2022; 13: 912933. https://doi.org/10.3389/fimmu.2022.912933.

[35] Zusso M, Lunardi V, Franceschini D, Pagetta A, Lo R, Stifani S, *et al*. Ciprofloxacin and levofloxacin attenuate microglia inflammatory response via TLR4/NF-kB pathway. Journal of Neuroinflammation. 2019; 16: 148. https://doi.org/10.1186/s12974-019-1538-9.

[36] Puppala ER, Prasad N, Prakash AN, Abubakar M, Syamprasad NP, Gangasani JK, *et al*. Mesua assamica (King & Prain) kosterm. bark ethanolic extract attenuates rheumatoid arthritis via down-regulating TLR4/NF-κB/COX-2/iNOS and activation of Nrf2/HO-1 pathways: A comprehensive study on in-vitro and in-vivo models. Journal of Ethnopharmacology. 2024; 335: 118671. https://doi.org/10.1016/j.jep.2024.118671.

[37] Werner LE, Wagner U. Calcium-sensing receptor-mediated NLRP3 inflammasome activation in rheumatoid arthritis and autoinflammation. Frontiers in Physiology. 2023; 13: 1078569. https://doi.org/10.3389/fphys.2022.1078569.